

ScRNA-seq Unveils the Functional Characteristics of Glioma-Associated Macrophages and the Regulatory Effects of Chlorogenic Acid on the Immune Microenvironment—A Study Based on Mouse Models and Clinical Practice

[Jiachen Wang](#) , [Shenglan Li](#) , [Yuxiao Chen](#) , Jinyi Chen , Can Wang , Zhuang Kang , Mengqian Huang , Zehao Cai , Yuxiang Fan , Yanjie Lan , [Yumeng Yu](#) , Ruining Bai , [Feng Chen](#) , [Wenbin Li](#) *

Posted Date: 6 August 2024

doi: 10.20944/preprints202408.0392.v1

Keywords: Chlorogenic acid; Glioma; Tumor-associated macrophages; Microglia; Immune microenvironment; Single-cell sequencing; Network pharmacology



Preprints.org is a free multidiscipline platform providing preprint service that is dedicated to making early versions of research outputs permanently available and citable. Preprints posted at Preprints.org appear in Web of Science, Crossref, Google Scholar, Scilit, Europe PMC.

Copyright: This is an open access article distributed under the Creative Commons Attribution License which permits unrestricted use, distribution, and reproduction in any medium, provided the original work is properly cited.

Article

ScRNA-Seq Unveils the Functional Characteristics of Glioma-Associated Macrophages and the Regulatory Effects of Chlorogenic Acid on the Immune Microenvironment—A Study Based on Mouse Models and Clinical Practice

Jiachen Wang ^{1,2,#}, Shenglan Li ^{1,#}, Yuxiao Chen ^{1,2,#}, Jinyi Chen ^{1,3}, Can Wang ¹, Zhuang Kang ¹, Mengqian Huang ^{1,2}, Zehao Cai ^{1,5}, Yuxiang Fan ⁴, Yanjie Lan ¹, Yumeng Yu ^{1,2}, Ruining Bai ^{1,2}, Feng Chen ¹ and Wenbin Li ^{1,*}

¹ Department of Neuro-oncology, Cancer Center, Beijing Tiantan Hospital, Capital Medical University, No.119, West Nan Si Huan Road, Fengtai District, Beijing, 100071, China.

² Capital Medical University, Beijing, 100069, China

³ Capital Medical University, Chinese Institute for Brain Research, Beijing, 102206, China

⁴ Department of Neurosurgery, Capital Medical University Xuanwu Hospital, Beijing, 100053, China

⁵ Department of Hematology, Xuanwu Hospital, Capital Medical University, Beijing, 100053, China.

* Correspondence: liwenbin@ccmu.edu.cn

These authors contributed equally to this work and should be considered co-first authors.

Simple Summary: This research is to elucidate the subpopulations and functional characteristics of tumor-associated macrophages, to dissect the regulatory effects of chlorogenic acid on the immune microenvironment, and to assess its clinical application potential. Utilizing scRNA-seq, the heterogeneity and differentiation trajectory of TAMs, encompassing bone marrow-derived suppressor monocytes and microglia, have been delineated. It is demonstrated that chlorogenic acid significantly attenuates glioma progression and extends the survival of the murine model. The regulatory influence of chlorogenic acid on TAMs has been meticulously investigated, revealing its capacity to activate microglia via the JAK-STAT signaling pathway. This finding is validated through PPI and molecular docking, leveraging data from public databases. A case of a patient treated with chlorogenic acid was reviewed, who survived for 5 years and 6 months, achieved partial remission after 9 months of treatment, and remains alive with no new symptoms or toxic side effects.

Abstract: Glioma is the most common primary malignant brain tumors. Despite advances in surgical techniques and treatment regimens, the therapeutic effects remain unsatisfactory. Immunotherapy has brought new hope to glioma patients, but the immunosuppressive nature of the tumor microenvironment (TME) has limited the therapeutic outcomes. This study aims to reveal the subpopulations and functional characteristics of tumor-associated macrophages (TAMs), to explore the regulatory effects of chlorogenic acid on the immune microenvironment, and investigate its potential for clinical application. In this study, Chlorogenic acid slowed tumor growth in the mouse model and extended the survival time of the mice. ScRNA-seq analysis elucidated the differentiation trajectories and functional characteristics of BMDMs and microglia, revealing the regulatory effects of chlorogenic acid on these two populations. It enhanced the antigen-presenting function of macrophages and the gene expression related to T-cell immune activation, activated microglia through the JAK-STAT pathway, and improved antitumor functions. Using the target prediction database, a PPI and molecular docking model were constructed, confirming the good affinity of chlorogenic acid with STAT1. A case of a patient treated with chlorogenic acid was reviewed, who survived for 5 years and 6 months, achieved partial remission (PR) after 9 months of treatment, and remains alive with no new symptoms or toxic side effects. Our study revealed the subtypes and differentiation trajectories of tumor-associated macrophages. Chlorogenic acid significantly improved the immune microenvironment of glioma by modulating the function of

bone marrow-derived mono-macrophages (BMDMs) and microglia, demonstrating good antitumor effects. This study provides new insights for targeting the regulation of the TME and offers theoretical and practical support for the clinical application of chlorogenic acid.

Keywords: chlorogenic acid; glioma; tumor-associated macrophages; microglia; immune microenvironment; single-cell sequencing; network pharmacology

1. Introduction

Glioma is the most common primary malignant brain tumor in adults, accounting for approximately 30% of all primary brain tumors and 80% of malignant brain tumors [1]. Glioblastoma (GBM) is the most common and aggressive subtype, and its standard treatment includes surgical resection, radiotherapy, and chemotherapy. However, despite advancements in surgical techniques and treatment protocols, the prognosis for GBM remains poor [2]. At present, the only specific drug used for the treatment of GBM is temozolomide, and its efficacy is still not satisfactory.

In recent years, immunotherapy, as a novel therapeutic approach, has brought hope to patients with GBM. The main types of immunotherapies include immune checkpoint inhibitors (such as PD-1 and PD-L1 inhibitors/antibodies), chimeric antigen receptor T-cell therapy (CAR-T), and oncolytic virus therapy, among others [3,4]. However, due to the highly immunosuppressive nature of the tumor microenvironment (TME) in GBM, coupled with the relatively low selective permeability of the blood-brain barrier and the heterogeneity of tumor cells, the efficacy of these treatment modalities is often limited [3].

TME, composed of blood vessels surrounding tumor cells, immune cells, stromal cells, extracellular matrix, and other signaling molecules [5], has been recognized as a dynamic interplay of components that collectively respond to the growth needs of tumor cells, becoming one of the main reasons for tumor progression and drug resistance [5]. Among them, tumor-associated macrophages (TAMs) are the most critical cell population. Broadly speaking, TAMs include tissue-resident macrophages (microglia, MG), bone marrow-derived monocytes (BMDMs), polarized macrophages (M1/M2), and dendritic cells (DCs) [6]. Generally, TAMs usually refer to inhibitory polarized macrophages (M2) or tumor-Infiltrating myeloid suppressive cells, which are the main culprits of immunosuppression in the TME [7]. They can enhance the stemness, proliferation, survival, and migration abilities of tumor stem cells (GSCs), while suppressing adaptive immune responses and having extensive symbiotic relationships with tumor cells. Several drugs targeting TAMs have been developed, including CSF-1R inhibitors, CCL2/CCR2 blockers, and CD47-SIRP α modulators [8]. These drugs show some promise in other types of cancer, but in the immune microenvironment of glioma, the complexity and diversity of TAMs make the effects of these treatment methods less satisfactory.

Chlorogenic acid (CHA, CGA, CA), also known as 5-O-caffeoylquinic acid, is a natural phenolic acid produced by plants such as tea leaves and coffee beans, and its safety has been recognized [9,10]. Previous studies have shown that chlorogenic acid has a wide range of biological activities, such as antimicrobial, immunomodulatory, antioxidant, and anticancer properties, which can reduce the risk of various diseases [11,12]. Chlorogenic acid modulates the cell cycle through multiple mechanisms or promotes cell death through other pathways, exerting cytotoxic effects [13–15]. Recent research has found that chlorogenic acid can induce differentiation in a variety of cancer cells, including glioma cells, reducing the malignancy of tumor cells, and its therapeutic effect in animal experiments is comparable to that of temozolomide [10]. Chlorogenic acid has also shown a positive effect on improving the immunosuppressive nature of the tumor microenvironment (TME) in glioma.

Our laboratory has been dedicated to the study of chlorogenic acid's anti-glioma effects. Our early research indicated that chlorogenic acid can activate the JAK-STAT pathway, inducing macrophages to polarize into the M1 rather than M2 phenotype, thereby exerting anti-tumor effects [16,17]. Recent studies have found that chlorogenic acid downregulates the expression of PD-L1

through the STAT1-IRF1 pathway, promoting the infiltration and activation of memory T cells and effector T cells near tumor tissues, and enhancing the efficacy of PD-1 antibodies [18,19]. Chlorogenic acid has now entered the clinical trial phase. The results of a study on the efficacy and safety of chlorogenic acid in treating high-grade gliomas (CTR20160113) have shown that chlorogenic acid has good safety and has provided preliminary clinical benefits for patients with high-grade gliomas who have relapsed after receiving standard therapy [20].

Nevertheless, our understanding of the mechanisms by which chlorogenic acid treats gliomas, especially its targeting effects on the immune microenvironment, is still limited. In this study, we re-examined the development and differentiation trajectories of tumor-infiltrating myeloid cells and microglia, and conducted an in-depth investigation of the effects of chlorogenic acid on the immune microenvironment of gliomas. This provides new insights for TAMs and regulating TME. At the same time, we report clinical data on the treatment of recurrent glioma patients with chlorogenic acid for the first-time, serving as an important basis for the therapeutic effects of chlorogenic acid.

2. Materials and Methods

Anti-Cancer Drugs

Chlorogenic acid was acquired from the Jiuzhang Biochemical Engineering Science and Technology Development Co., Ltd. (Chengdu, Sichuan, China), which with a purity of more than 99%. CGA was dissolved in normal saline (NS) at a concentration of 100 mM as a stock solution for in vivo experiment.

Orthotopic Transplantation Model in C57BL6/N Mice

To investigate the in vivo anti-glioma effects of chlorogenic acid, we selected female C57BL6/N mice aged 6 weeks and weighing between 15 to 20g. The GL261-Luc cells labeled with luciferase were used to establish the orthotopic glioma transplantation model, and the anti-tumor effect was detected using an in vivo imaging system. The GL261-Luc cell line was digested with trypsin and resuspended in PBS solution to adjust the density to $1.5 \times 10^5/5 \mu\text{L}$ and kept on ice for later use. Immunocompetent C57BL6/N mice were anesthetized by intraperitoneal injection of tribromoethanol, and the ear bar was inserted into the external auditory meatus of the mouse to adjust the position of the incisor bar of the positioning device to be $3.3\text{mm} \pm 0.4\text{mm}$ below the horizontal line, ensuring that the mouse's skull was in a horizontal position. Subsequently, surgery was performed on the skin of the mouse's head. Under the guidance of the stereotactic apparatus, with the anterior fontanelle as the origin, the needle was inserted vertically 3mm at the position 2mm behind the anterior fontanelle and 2mm lateral to the midline, slightly pulling back the needle about 0.5mm before injection, and the GL261-Luc single-cell suspension was injected at a speed of $2.5 \mu\text{L}/\text{min}$ through a micro pump. After injection, the needle was kept in place for 1 minute, then retracted, the puncture hole was sealed with bone wax, and the scalp wound was finally disinfected with iodine and sutured.

Three days after inoculation, the surviving mice were photographed in the in vivo imaging system and randomly divided into the experimental group and the control group (6 mice per group). The experimental group was injected with chlorogenic acid (40mg/kg) intraperitoneally every day, and the control group was injected with physiological saline (40mg/kg) intraperitoneally every day. The setting of this dose was referred to previous studies [16]. On the 7th, 14th, and 21st days after inoculation, the activity and mental state of the mice were observed, and tumor growth was recorded in the in vivo imaging system, and the survival days of mice in the control and experimental groups were recorded. The tumor inhibition effect of chlorogenic acid was evaluated by calculating the bioluminescence values.

Single-Cell RNA-Seq Data Preprocessing and Normalization

Raw sequencing data were demultiplexed and converted into fastq format using CellRanger v3.0.1 (10× Genomics) and Illumina [21,22]. The sequencing results were mapped to the mouse genome GRCm38 (mm10) obtained from the 10× Genomics website and quantified using CellRanger.

A total of 35,359 cells were identified by CellRanger. Data analysis was performed using Seurat (v4.4.0) in R [23]. Unless specifically stated in our methods, all other quantitative parameters were set to default values. To filter out possible empty droplets, low-quality cells, and possible multiple droplets, we set the following thresholds to remove low-quality cells (Cell-level filtering): 1. Cells with transcripts less than 200 or more than 3000; 2. UMI counts greater than 500 per cell; 3. More than 500 genes detected per cell; 4. Mitochondrial count percentage less than 0.2; 5. We calculated the complexity using $\log_{10}(\text{GenesPerUMI})$ and selected cells with a complexity greater than 0.80 to exclude low-complexity cell type contamination. Additionally, we performed gene-level filtering (Cell-level filtering), where we removed genes with zero expression in all cells, retaining only those expressed in 10 or more cells. After the above filtering, a total of 25,334 cells in the dataset proceeded to the next steps of the process.

We performed Harmony integration [24] and differential normalization on each sample, and regressed out unwanted variations such as mitochondrial genes, ribosomal genes, and cell cycle genes. The gene expression measurements for each cell were normalized by multiplying the total number of transcripts within the cell by the default scaling factor, and the normalized values were log-transformed (using the "LogNormalize" method). Following the Seurat workflow, variance-stabilizing transformation ("vst") was used to identify the 2000 most variable genes across each replicate. Principal component analysis (PCA) was applied for dimensionality reduction of the data, a nearest-neighbor graph was constructed using the neighbor function, and an unsupervised clustering algorithm was applied using the Louvain function (resolution = 0.4). The dimensionality reduction results were projected onto a two-dimensional plane using UMAP.

Cell Annotation and Differential Gene Analysis

After identifying immune cells, monocyte-macrophages, microglia, T cells and NK cells, and B cells based on the report/canonical scRNA markers of different types of cells (Table S1), we repeated the aforementioned clustering steps for further study. We used the Wilcoxon rank-sum test provided by Seurat to study the characteristic upregulated/downregulated genes between different cell subpopulations and groups, and further performed GSEA analysis on these genes. The GSEA analysis was conducted in the R package clusterProfiler (v4.6.2) [25]. We used the Gene Ontology: Biological Process (GO:BP) and Reactome databases built into clusterProfiler to analyze the biological characteristics of the differential genes [26]. GO annotation for mice was performed using the org.Mm.eg.db (v3.4.0) package [27]. Redundant results were also eliminated using the simplify function (cutoff = 0.7).

Pseudotime Analysis with Monocle3

Monocle 3 (v3.1.4) is a tool for single-cell RNA sequencing data analysis that can identify transitions and trajectories of cellular states [28]. We used PCA for dimensionality reduction prior to pseudotime analysis, with the PC values consistent with the parameters used for dimensionality reduction clustering in Seurat. Unless specifically stated in our methods, all other quantitative parameters were set to default. The parameters for Monocle3 were all set to their default values. In identifying the starting point of pseudotime (learn_graph), we manually delineated based on the biological significance of the cell subpopulations and the minimum value of the 'pseudotime' parameter, and the results were returned to Seurat for further analysis.

Gene Set Variation Analysis (GSVA)

GSVA is a non-parametric, unsupervised algorithm that is centered on gene sets and can transform a gene expression matrix into an expression matrix based on gene sets. We compared the similarity between the two groups of differential genes, CHA-Deg and Act-Deg, using the R package GSVA [29].

Obtaining Network Pharmacology-Related Targets

The chemical structure of chlorogenic acid (Canonical SMILES) was obtained through PubChem [30] (<https://pubchem.ncbi.nlm.nih.gov/>). The SMILES results were then imported into the SwissTargetPrediction database [31] (<http://www.swisstargetprediction.ch/>) and the SuperPred database [32] (<https://prediction.chlorogenicacid.rite.de/>) to predict compound targets, and the results from both databases were integrated. Keywords related to glioma and microglia polarization: We used the keywords "glioma" and "microglia activation" to obtain network pharmacology targets related to the disease and microglia in the OMIM database [33] (<http://www.omim.org/>) and the GeneCards database [34] (<http://www.genecards.org/>), respectively, and integrated the results from these two databases.

Constructing Protein-Protein Interaction (PPI) Networks and Topological Analysis

To investigate the role of microglia in the glioma treatment process with chlorogenic acid, we imported candidate targets into the STRING (v12.0) (<https://string-db.org/>). We constructed a PPI network, which was subsequently visualized using Cytoscape (v3.10.1). To obtain topological parameters, we calculated the clustering coefficient, node degree distribution, shortest path, and length distribution using the network analyzer settings. The network was analyzed using "Analyze Network" in Cytoscape. The size and color of each node were set to reflect the degree of influence on the comprehensive score, thereby obtaining the final PPI network. Additionally, we performed cluster analysis on the PPI network using 11 algorithms based on the Cytohubba [35] (including MCC, DMNC, MNC, Degree, EPC, BottleNeck, Eccentricity, and Closeness) to extract core gene modules.

To further study the spatial conformation of the binding between chlorogenic acid and its core targets, we obtained the 3D structural files of chlorogenic acid and the core target STAT1 from the TCMSP database [36] (<https://old.tcmsp-e.com/tcmsp.php>) and the Protein Data Bank database [37] (<https://www.rcsb.org/>), respectively. Molecular docking was performed using Discovery Studio (<https://www.3ds.com/products/biovia/discovery-studio>) to obtain the binding energy and visualize the docking situation.

3. Results

3.1. The Tumor Suppression Effect of Chlorogenic Acid on the Transplantation Model

To investigate the effects of chlorogenic acid on the immune microenvironment of glioma in patients, we selected mice of the C57BL6/N strain to construct an orthotopic GL261 glioma model, which more closely simulates the immune microenvironment of human glioma. Using small animal in vivo imaging technology, we quantitatively analyzed and evaluated the tumor growth in the mouse model. In the experimental group treated with chlorogenic acid, we observed a significant reduction in luminescence intensity, which represents tumor size, compared to the control group ($p < 0.001$) (Figure 1A). In the control group, where mice were treated with saline injections, we recorded a significant increase in tumor volume by day 14 compared to day 7, and all mice in the control group died within 21 days of the experiment. In contrast, the chlorogenic acid-treated group showed a significant survival advantage: more than half of the mice were still alive by day 14, and half were able to survive until day 21 (Figure 1B,C). These results suggest that chlorogenic acid not only significantly inhibits the growth of orthotopically transplanted glioma in mice but also improves the survival rate of mice with glioma.

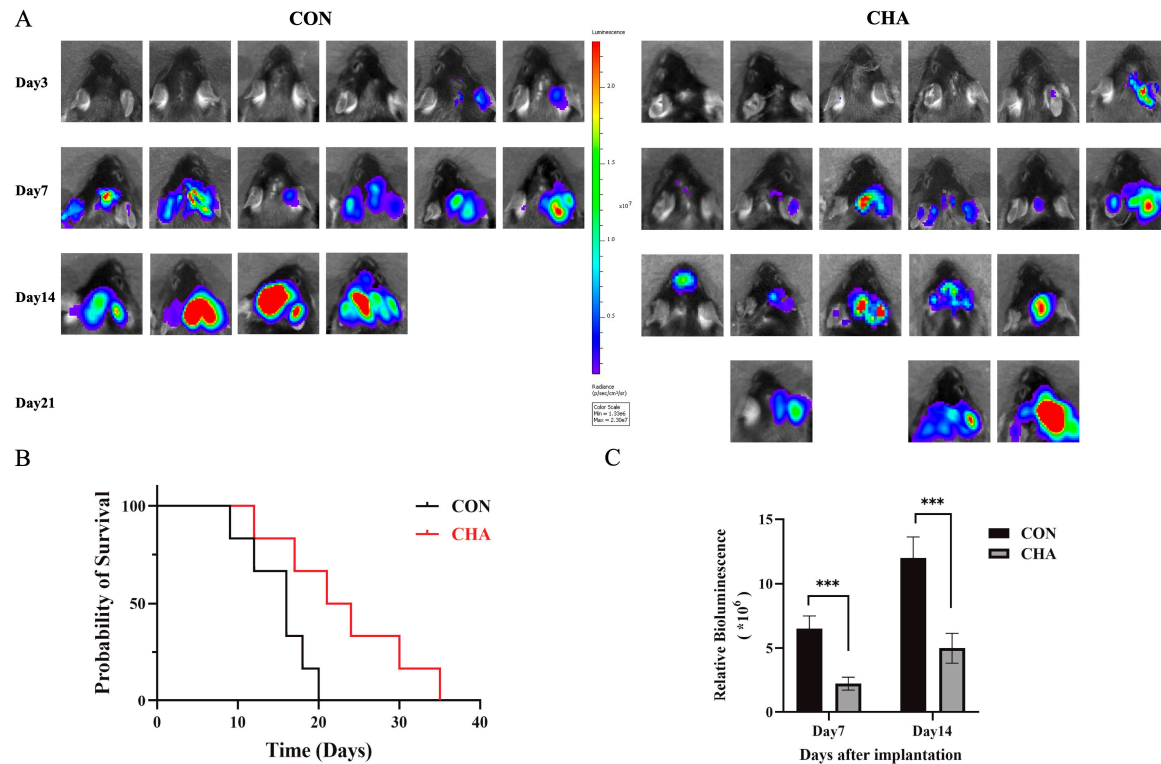


Figure 1. Effect of chlorogenic acid on GL261-luc tumor model in immunized normal mice (C57BL6/N). (A) Biological in vivo imaging of mice in experimental and control groups on days 3, 7, 14 and 21 of inoculation. (B) Survival curves of experimental and control groups. (C) Tumor size statistics of experimental and control groups on day 7 and 14 ($p < 0.05$).

3.2. Single-Cell Atlas of GL261 Glioma-Microenvironment under the Influence of Chlorogenic Acid

We performed scRNA-seq analysis on mixed tumor tissues from three experimental mice treated with chlorogenic acid for 14 days and three control mice, to investigate the impact of chlorogenic acid on the immune microenvironment of mouse glioma. After quality control, a total of 25,334 cells were analyzed, detecting 18,634 expressed genes (Supplement Figure S1). We used unsupervised clustering analysis to categorize the cells into 19 clusters and displayed the high-dimensional data on a two-dimensional plane using UMAP (**Error! Reference source not found.A**). Among the annotated 22,262 immune cells ($Ptprc^+$), we identified a substantial number of infiltrating T or NK cells ($Cd2^{hi}$, $Cd3d^{hi}$, $Cd3e^{hi}$). These immune cells also included a significant number of tumor-associated macrophages ($Tgfb^{hi}$, $Ifitm2^{hi}$, $Ifitm3^{hi}$) and a small number of B cells ($Cd79a^{hi}$, $Cd19^{hi}$, $Ms4a1^{hi}$) (**Error! Reference source not found.B,C**). We distinguished the TAMs population into central microglia and bone marrow-derived populations using $CD49a$ ($Itga4$), identified microglia using classical markers $Tmem119$, $Crybb1$, and $P2ry12$, preliminarily identified the Mo/M ϕ fraction using monocyte markers $Chil3$, $Plac8$, and macrophage markers $Ifitm2$, $S100a6$, and $S100a11$, and identified dendritic cells DCs using $Cd24a$ and $Ly75$ (**Error! Reference source not found.D,E**) [38–40].

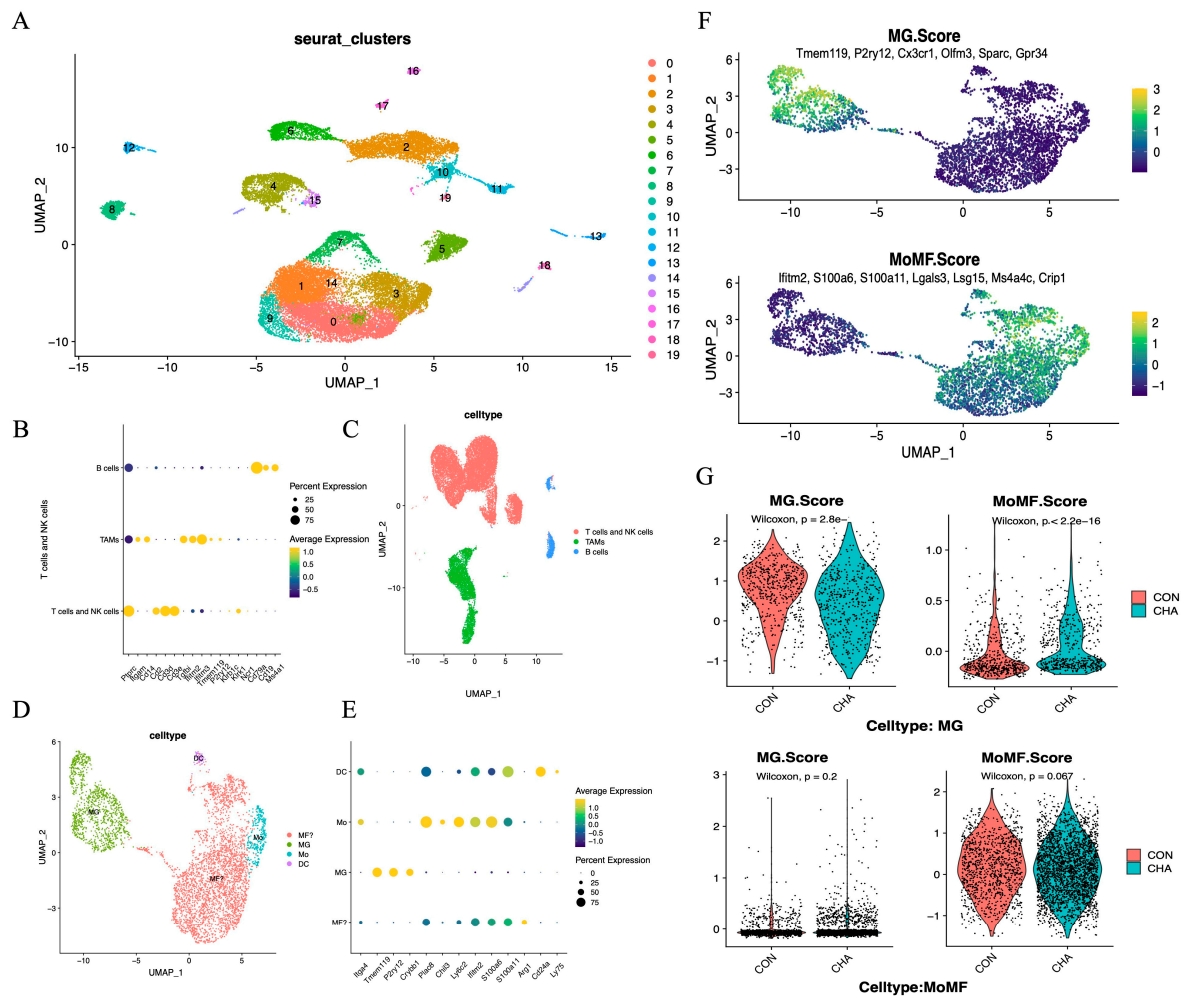


Figure 2. scRNA-seq reveals tumor microenvironmental mapping. (A) UMAP showing microenvironmental mapping of glioma tissues from 3 experimental and 3 control mice. (B) Marker for B cells, T cells/NK cells, and MG/monocyte systems. (C) Distribution of subpopulations of immune cells (Ptprc+). (D) UMAP plot showing innate immune cell mapping. (E) Marker for four types of cells, dendritic cells (DC), monocytes (Mo), microglia (MG), and monocyte-macrophages (MF). (F) Scores of microglia feature scores and macrophage feature scores in innate immune cells. (G) Violin plots demonstrating the two scores for experimental and control groups in macrophages and microglia, respectively.

To further investigate the influence of chlorogenic acid on the two main populations of TAMs, we employed MG scores and MoMF scores designed by the average expression levels of specific genes (**Error! Reference source not found.**F,G and Table S1). Our analysis showed that these scores effectively differentiated the two cell populations. After treatment with chlorogenic acid, the MG score of the microglial population decreased, while the MoMF score significantly increased ($p<0.05$), indicating that microglia may have undergone a shift towards macrophage characteristics. In contrast, the macrophage population maintained a low MG score after chlorogenic acid treatment, and the MF score did not change significantly ($p>0.05$), which may reflect that the mechanism of action of chlorogenic acid on the macrophage population is different from that on microglia and involves a more complex regulatory process.

3.3. Reconstructs the Differentiation Trajectory of BMDMs

Tumor-associated macrophages (TAMs) are a highly heterogeneous group of cells in the human glioma microenvironment. BMDMs infiltrate from the bloodstream into the tumor tissue, becoming part of the TAMs, and differentiate into phenotypes with different functions under the stimulation

of specific signals in glioma. In scRNA-seq, we considered the BMDMs as a continuum and identified six subgroups within this population (**Error! Reference source not found.**A,B). We determined monocytes (Ly6c^{hi}, Sell^{hi}, Ccr2^{hi}, Plac8^{hi}, Tgfb^{low}), to the transitional state intMoMF (Ly6c^{hi} and Tgfb^{hi}), and then to functionally differentiated macrophages TAM1 (Il1b^{hi}, MHC-II^{hi}), TAM2 (Arg1^{hi}), and TAM3 (Gpnmb^{hi}, Apoe^{hi}), as well as dendritic cells DCs (Cst3⁺, Cd24a⁺, MHC-II^{hi}).

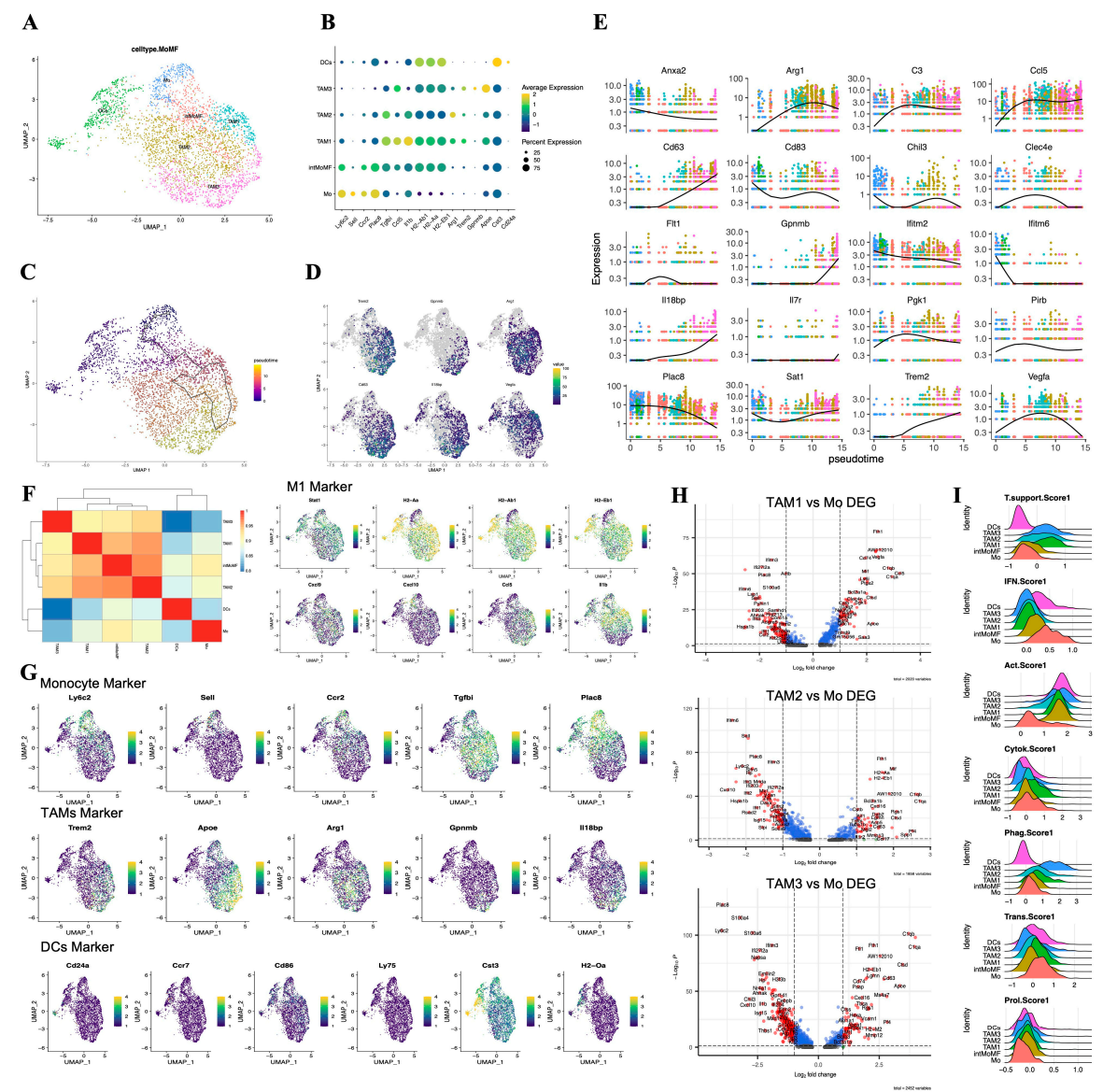


Figure 3. Subpopulation heterogeneity of monocyte-macrophages. (A) UMAP plot demonstrating single-cell mapping of monocyte-derived subpopulations. (B) Marker of monocyte-derived subpopulations. (C) Pseudotime differentiation trajectory of monocyte-macrophages. (D) Key genes of immunosuppressive differentiation trajectories. (E) Trajectory node genes of monocyte-macrophage differentiation. (F) Heatmap demonstrating Spearman correlation between different cell subpopulations Spearman's correlation. (G) UMAP plot demonstrating key markers for monocytes, suppressor macrophages, M1 macrophages and DCs. (H) Differential genes of TAM1, TAM2, TAM3 subpopulations compared to monocyte Mo (p<0.05). (I) Ridge plot indicating the degree of tumor-supporting, the degree of activation of the IFN pathway, tumor activation degree, degree of cytokine secretion, phagocytosis, expression of transcription factors and cell proliferation of different cellular subpopulations (see Table S1 for scoring genes).

Through pseudotime analysis, we depicted the differentiation trajectory of the BMDMs in the glioma microenvironment (**Error! Reference source not found.**C–E). High expression of Cd83, Chil3,

and Plac8 in Mo are the earliest time markers, accompanied by the activation of the inflammatory response pathway interferon (IFN) (Ifitm6, Ifitm2). Over time, the expression of these inflammatory genes rapidly declines, while factors that promote tumor growth, such as Vegfa and Arg1 that promote tumor angiogenesis and the signature genes Trem2 and Apoe that promote tumor growth, continue to rise. Eventually, the expression of Gpnmb and Il18bp rises, marking the 'hijacking' of the TAMs population by glioma cells is complete, and these results are consistent with the research conclusions of Daniel et al. [40].

Furthermore, we used Spearman correlation analysis to explore the correlation between gene expressions of various cell subgroups and presented it through a heatmap (**Error! Reference source not found.F**). We can see that Mo maintains a certain correlation with both DCs and TAMs on either side, while there is a stronger correlation among the internal subgroups of macrophages, which is consistent with the conclusions of pseudotime analysis. Among the three subgroups of TAMs, we observed that these cells have higher scores for tumor activation (MHC-II, Cd52) and phagocytic function (Apoe, Lgals5), indicating that these TAMs still have certain antigen presentation capabilities (**Error! Reference source not found.I** and Table S1). Compared to Mo, the expression of complement-related genes (C1qa, C1qb) and lysosomal cathepsins in TAMs increased (Ctss, Ctsd). In addition to the decline in the expression of IFN pathway-related genes (Il1b, Ifitm2, Ifitm3, Ifi204) and monocyte marker genes (Ly6c2, Plac8), we also found that the expression of genes encoding calcium-binding proteins (S100a4, S100a6, S100a10) and the gene encoding chemokine Cxcl10 also declined ($p < 0.05$, $\log_2FC = 1$) (**Error! Reference source not found.H**). Among them, TAM1 has a relatively stronger M1 polarization trend, while TAM3 has a more comprehensive expression of immunosuppressive genes (**Error! Reference source not found.G**). These results facilitate our next step in exploring the effects of chlorogenic acid on TAMs and provide a new perspective for understanding the complexity of glioma microenvironment.

3.4. The Regulatory Effect of Chlorogenic Acid on the Transcriptional Characteristics of BMDMs

Our laboratory previously explored the regulatory effect of chlorogenic acid on macrophages using animal models and discovered the potential of chlorogenic acid to re-polarize M2-type macrophages to the M1 phenotype [16]. To further investigate the regulatory effect of chlorogenic acid on tumor-associated macrophages and the mechanisms behind it, we employed GSEA to explore the activated gene networks after the action of chlorogenic acid and analyzed the differential genes through GO:BP and Reactome pathway databases (Table S4).

Our results showed that multiple biological pathways highly related to adaptive immune modulation were upregulated in the experimental group treated with chlorogenic acid compared to the control group. Among the significantly upregulated pathways were those directly related to adaptive immunity, such as antigen processing and presentation of peptide antigen (GO:0048002), retrograde protein transport, ER to cytosol (GO:0030970), endoplasmic reticulum to cytosol transport (GO:1903513), protein exit from endoplasmic reticulum (GO:0032527), and several pathways related to amino sugar and lipid metabolism (GO:0006040, GO:0034433, GO:0034434, GO:0034435) (**Error! Reference source not found.A,D**). Additionally, we assessed the correlation between differential genes and adaptive immunity. The GSEA analysis results showed that genes such as MHC-II (H2-T23, H2-D1, H2-Aa), Pnp, and Hspa8 are involved in T cell immunity (GO:0001916) ($p < 0.05$) (**Error! Reference source not found.C**). We then performed Reactome pathway analysis on these differential genes, and the enriched pathways included the IGF signaling pathway (R-MMU-381426), antigen presentation (R-MMU-983170), and lipid metabolism involved in the regulation of immunity (R-MMU-6798695) (Figure 4B). In the comparison of differential genes in the TAM3 subgroup ($p < 0.05$, $\log_2FC > 0.25$), we observed significant upregulation of gene expression for MHC-II (H2-Ab1, H2-DMa, H2-Aa, Cd74), osteopontin (Spp1), and lysosomal proteins (Cstb, Cstd) ($p < 0.05$) (**Error! Reference source not found.E,F**). The upregulation of these molecules may reflect changes in the activation state of macrophages. They collectively participate in the immune system's surveillance and clearance of tumor cells by enhancing antigen presentation, regulating adaptive immune

responses, and participating in the remodeling of the extracellular matrix, providing new strategies and insights into molecular mechanisms for the immunotherapy of glioma.

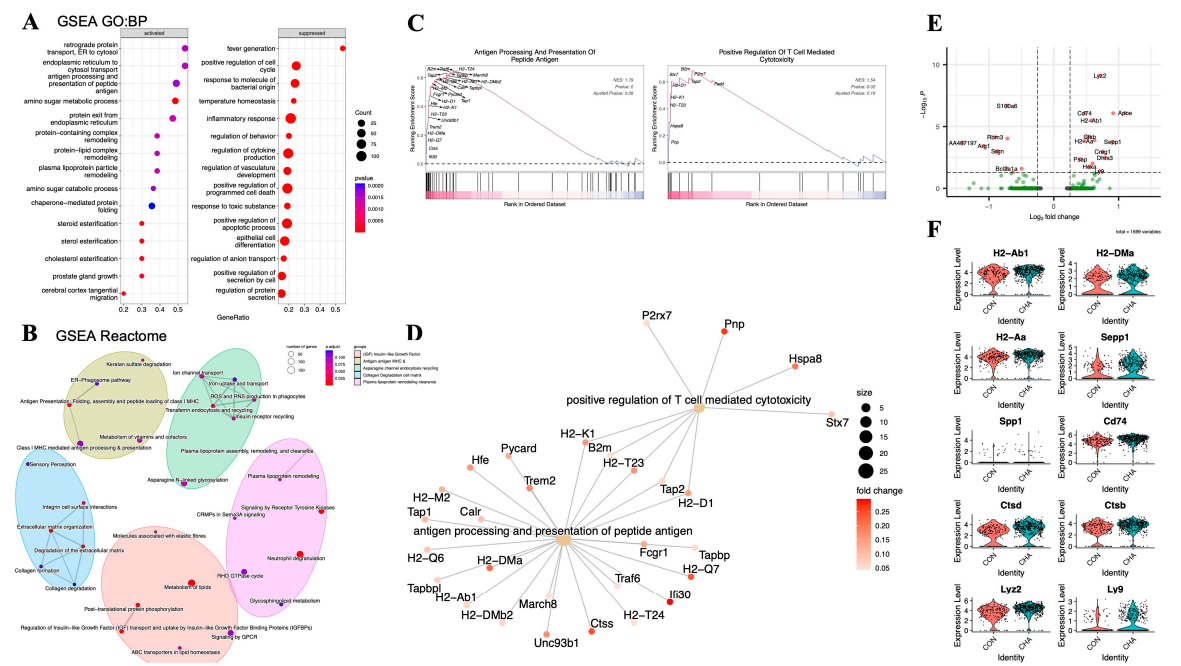


Figure 4. The functional effects of chlorogenic acid on monocyte-macrophages. (A) Bubble diagram showing the results of GO:BP analysis. (B) Network diagram showing the results of Reactome analysis. (C and D) GSEA plots and gene networks showing the GO:BP term: positive regulation of T cell mediated cytotoxicity and antigen processing and presentation of peptide antigen. (E) Volcano plot demonstrating the differentially expressed genes in the TAM3 subpopulation in the experimental group compared to the control group ($\log_2FC>0.25$, $P<0.05$). (F) Violin plot demonstrating the TAM3 in the experimental group Some of the differentially up-regulated genes.

3.5. The Anti-Tumor Activation Trajectory of Microglia

Based on the expression patterns of the microglial marker gene Tmem119 and MHC-II related genes, we divided microglia into two major subgroups: the homeostatic microglia Hom-MG (Tmem119^{hi}, MHC-II^{low}) and the activated microglia Act-MG (Tmem119⁺, MHC-II^{hi}). We reconstructed the anti-tumor response process of microglia under glioma activation, which showed a series of gene changes involved in the activation process of microglia (**Error! Reference source not found.**A–C): including the enhancement of MHC-II gene expression (H2-Aa, H2-Ab1, H2-Eb1, Cd74, B2m), activation of the IFN pathway (Ifitm3, Ifi2712a, Ifit2, Ifit3), activation of the complement system (C4b), and the weakening of inhibitors of the NFkB pathway (Nfkb1, Nfkbia, Nfkbiz, Tnfaip3).

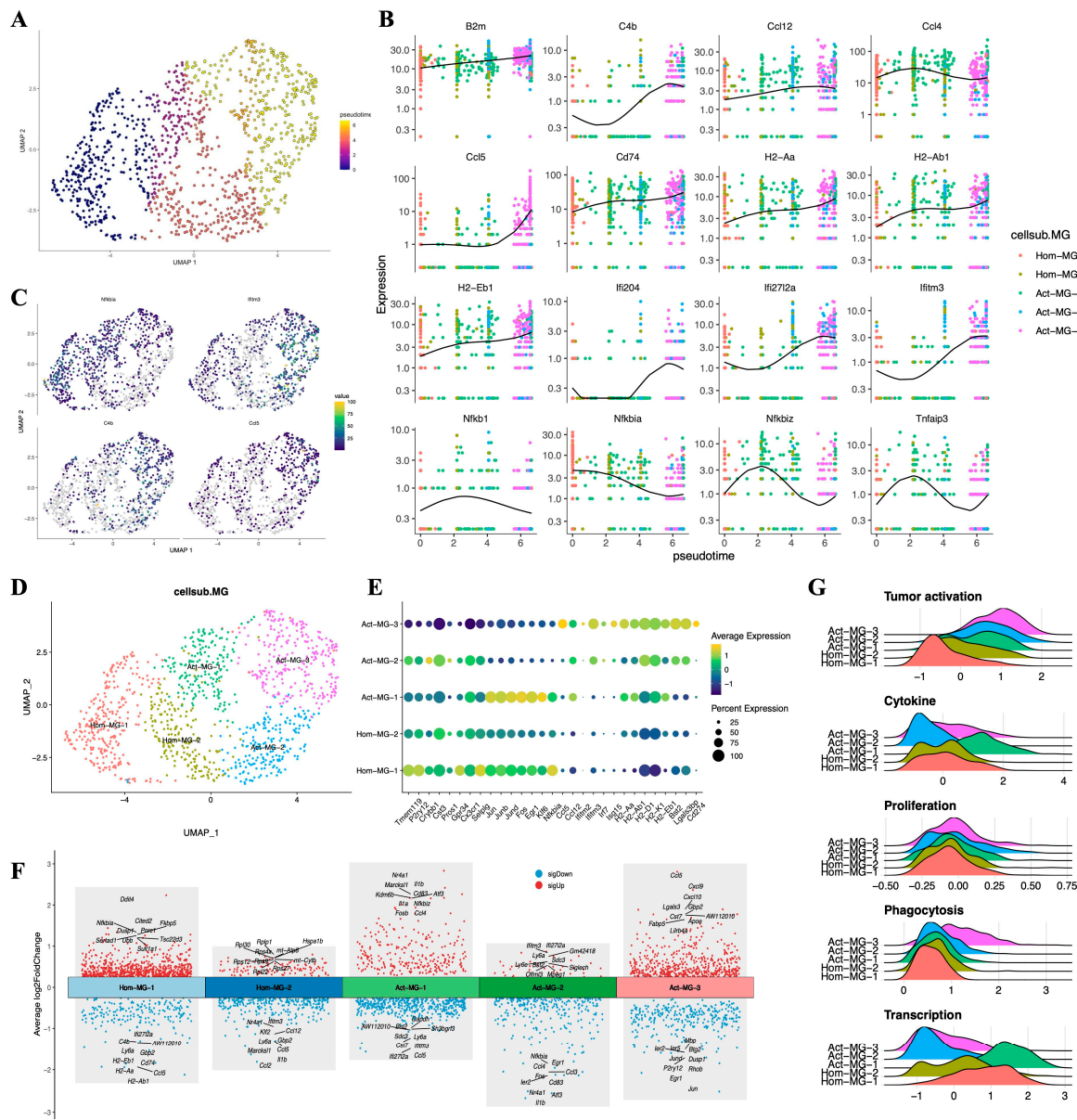


Figure 5. Differentiation trajectories and functional characteristics of microglia. (A) Pseudotime differentiation trajectories of microglia. (B) Trajectory node genes for microglia activation. (C) Expression changes of Nfkbia, Ifitm3, C4b, and Ccl5 genes during microglia activation. (D) Subpopulation mapping of microglia. (E) Expression of marker genes in microglia subpopulations. (F) Multi-group volcano plot representing the top 10 differential genes of each microglia subpopulation sorted according to decreasing log2FC (log2FC > 0.5, p < 0.05). (G) Tumor activation, cytokine expression, cell proliferation capacity, phagocytosis, and expression of transcription factors of each subpopulation of microglia (see Table S1 for scoring genes).

Through differential expression analysis (p<0.05, log2FC>0.25), we further delineated the transcriptional characteristics of these subgroups (Error! Reference source not found.D–F). The Hom-MG-1 subgroup highly expressed the innate characteristic genes of microglia (Tmem119, P2ry12, Crybb1, Cst1, Gpr34, Cx3cr1), with lower expression levels of tumor activation-related genes, and expressed early activation genes to a certain extent (Jun, Junb, Jund, Fos), suggesting that these cells are homeostatic microglia that have not yet been activated by the tumor but have the potential to activate. The Hom-MG-2 cluster showed a mixed expression pattern of homeostatic genes, transcription factors, and tumor activation genes, indicating that these cells are in a state of dynamic change. Act-MG-1, on the basis of expressing MHC-II, significantly upregulated a series of transcription factors and cytokines (Ccl3, Ccl4, Jun, Junb, Jund), indicating that this cluster of cells is

a type of active microglia that quickly respond to tumor stimulation. The Act-MG-3 subgroup, however, showed high activity cells activated by the tumor, with strong phagocytic/lipid metabolic activity (Cst7, Apoe), but the expression of transcription factors and cytokines was weakened, indicating that these cells have been reprogrammed into polarized functional cells. It is worth noting that the expression of PD-L1 (Cd274) in the Act-MG-3 subgroup was upregulated, indicating that activated microglia are likely to have certain immunosuppressive properties, which is consistent with previous reports. In contrast, Act-MG-2 did not have such immunosuppressive characteristics but showed a more comprehensive transcriptional profile, indicating that these cells are in a transitional stage, similar to the Hom-MG-2 subgroup, but the degree of activation of MG-Act-2 seems to be higher (**Error! Reference source not found.**G and Table S1). These results reflect the process of microglia becoming more "macrophage-like," revealing the complex dynamics of microglia in the glioma microenvironment.

3.6. Chlorogenic Acid Promotes the Activation of Microglia

We further investigated whether chlorogenic acid is involved in the activation process of microglia. In the microglia of mice from the experimental group injected with chlorogenic acid, the "pseudotime scores" (Calculated by monocle3) were significantly higher than those of the control group, suggesting that chlorogenic acid can promote the transition of microglia to an activated state (**Error! Reference source not found.**A). We performed differential analysis on the microglia from both the experimental and control groups, obtaining sets of upregulated and downregulated genes, *MG_CHA_Deg* (**Error! Reference source not found.**B and Table S3). At the same time, we also analyzed the differential expression between the two subgroups of Act-MG and Hom-MG cells, obtaining the gene set *ActMG-Deg*. By calculating the Pearson correlation coefficient between these two sets of differentially expressed genes (**Error! Reference source not found.**C), we found that the changes in gene expression were highly synchronized ($R=0.9$, $p<2.2e-16$). To further corroborate this hypothesis, we used GSVA to analyze five different microglial subgroups and assess the expression of the chlorogenic acid-Deg gene set in these subgroups (**Error! Reference source not found.**D). The GSVA results showed that subgroup Act-MG-3 significantly enriched the expression of *MG_CHA_Deg*, while subgroup Hom-MG-1 had the lowest enrichment of *MG_CHA_Deg* ($P<2.2e-16$), which is consistent with our hypothesis that chlorogenic acid is involved in and promotes the activation process of microglia.

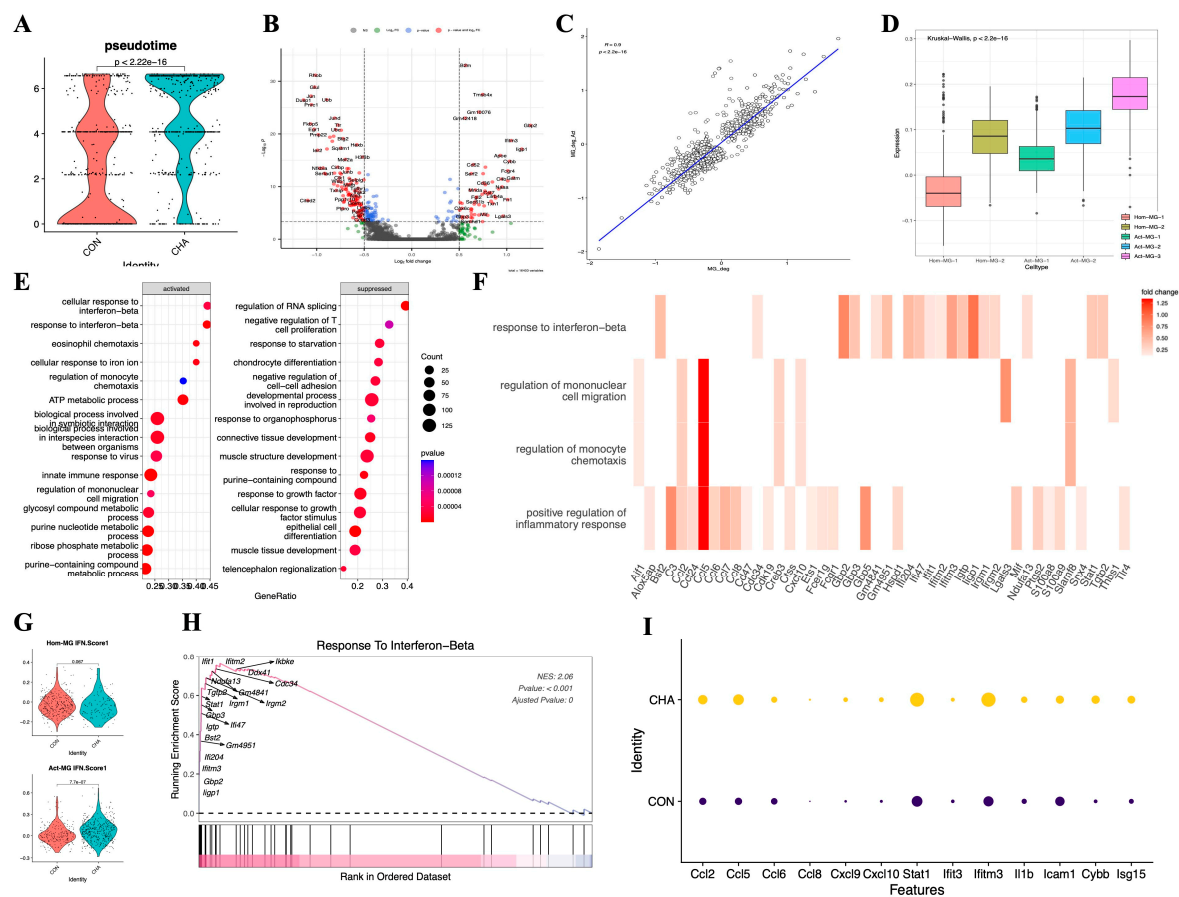


Figure 6. Effect of chlorogenic acid on microglia activation status. (A) Comparison of the difference in proposed chronological scores between chlorogenic acid experimental and control groups ($p < 0.05$). (B) Microglia differentially expressed genes in the experimental group compared to the control group. (C) Comparison of the differentially expressed genes (CHA-Deg) and the differentially expressed genes between microglia subpopulations of Act-MG and Hom-MG subpopulations of microglia between the groups (Act-Deg). Correlation between the two Deg genes. (D) GSVA analysis examined the degree of similarity between the differential genes in the two groups. (E) Differential genes in the experimental group compared to the control group, enrichment analysis GO:BP terms. (F) Heatmap showing the enriched genes in response to IFN- β , monocyte migration, modulation of monocyte chemotaxis, in response to inflammatory response GO:BP terms, the shade of the colors indicate the size of the difference in gene expression (fold change). (G) Comparison of the average expression of IFN pathway genes between the two populations Hom-Act and Act-MG, experimental and control. (H) GSEA plot in response to the IFN- β pathway. (I) Expression of genes downstream of chemokines and JAK-STAT.

We conducted GSEA analysis on the CHA-Deg differential gene set and enriched multiple upregulated or downregulated GO:BP terms (Error! Reference source not found.E,F). Among the upregulated pathways, the IFN regulation pathway (GO:0035456) was significantly enriched with the highest normalized enrichment score (NES=2.06). In addition, this differential gene set also significantly enriched pathways such as innate immune response (GO:0045087), complement pathway activation (GO:0006956), and monocyte migration (GO:0071675, GO:0071674). These upregulated pathways reflect that microglia show signs of activity and play an important role in immune regulation, metabolic control, and pathogen response. Most of the immune-related activation genes(Ccl2, Ccl5,6,7,8, Ccl24, Irgm1, 2, Gbp2, 3, 5,S100a8, S100a9) are directly involved in the production and signaling of IFN. The upregulation of Stat1 further emphasizes the importance of the JAK-STAT signaling pathway in this process. Furthermore, we focused on the differences in the activation degree of the IFN pathway between the Hom-MG and Act-MG cell populations (Error!

Reference source not found.G). The results showed that chlorogenic acid more significantly strengthened the response to the IFN pathway in the Act-MG population ($p<0.05$). We assessed several important downstream genes in this pathway (**Error! Reference source not found.H,I**), all of which showed enhanced expression, further emphasizing that chlorogenic acid regulates the immune response of microglia through the JAK-STAT pathway.

3.7. Cluster Analysis Based on PPI Network, Core Target Prediction, and Molecular Docking

We utilized the SwissTargetPrediction and Supred databases to predict the pharmacological targets of chlorogenic acid, identifying a total of 196 potential targets (**Error! Reference source not found.A**). Subsequently, we collected 3194 targets associated with glioma and 2558 targets related to microglial polarization from the OMIM and GeneCard databases. Using Venny to create a Venn diagram, we ultimately identified 68 candidate biological targets shared by chlorogenic acid and glioma (**Error! Reference source not found.B**). We then input these 68 candidate targets into the STRING database (confidence > 0.9) and used Cytoscape to draw a protein-protein interaction (PPI) network graph containing 45 targets and 77 edges (**Error! Reference source not found.C**). Employing 11 algorithms (see method) included in Cytoscape, we calculated the core targets, obtaining the effect values of each algorithm's results. By integrating the results of various algorithms, we selected nodes that appeared in at least 10 algorithms and ranked in the top 20 in the effect values of each algorithm as core genes (Table S2). Ultimately, we identified 16 core genes (**Error! Reference source not found.D**), including STAT1, SRC, CASP3, NFKB1, MMP9, TLR4, MAPK8, PRKCD, PIK3R1, MAPK1, MMP2, PRKCA, IKBKB, IGF1R, ITGB2, and PDGFRB. Among them, the STAT1 gene ranked the highest in the algorithm prediction, the result consistent with our GSEA enrichment analysis conclusions.

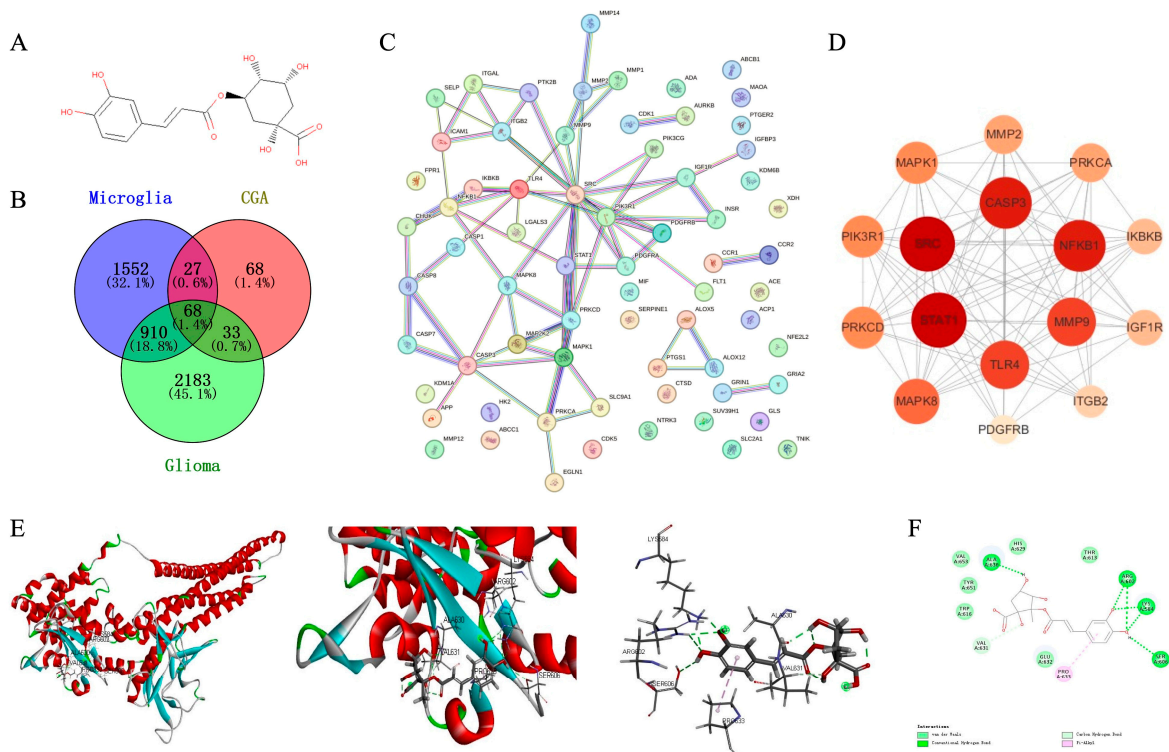


Figure 7. Construction of PPI network and molecular docking of chlorogenic acid in regulating microglia function. (A) Chemical structure of chlorogenic acid. (B) Common targets of microglia activation, chlorogenic acid and glioma. (C) Protein-protein interaction (PPI) network between 68 candidate biological targets. (D) Algorithmically optimized protein-interacting core genes. (E) 3D conformation showing the binding site of chlorogenic acid to STAT1 (marked in red), with the lowest

binding energy of -41.761 KJ/mol. (F) Van der Waals forces, hydrogen bonds and π -bonds in the binding site of chlorogenic acid and STAT1 are marked in light green, green and pink, respectively.

We conducted molecular docking of chlorogenic acid with STAT1 using Discovery Studio to simulate their binding spatial conformation (**Error! Reference source not found.**E,F). The results showed that the lowest binding energy was -41.741 kJ/mol, indicating that chlorogenic acid could adapt well to the active pocket of STAT1 and bind with multiple amino acid residues. These findings, from the molecular structural level, demonstrate the binding mode between STAT1 and chlorogenic acid, further confirming the potential of chlorogenic acid to modulate the downstream signaling of STAT1.

3.8. Clinical Application of Chlorogenic Acid in the Treatment of Recurrent Glioma Patients

We hereby report a clinical application of chlorogenic acid in the treatment of patient with recurrent glioma, along with imaging data for the first time. The patient was histologically diagnosed with WHO Grade 4 astrocytoma, IDH-mutant (IDH1 R132H mutation, MGMT promoter methylation, 1p19q codeletion, TERT C250T mutation, TERT C228T wildtype, IDH2 wildtype, BRAF wildtype), and experienced two recurrences after surgery and concurrent chemoradiotherapy, with intolerance to temozolomide (TMZ) during the treatment process. In June 2021, the patient was administered chlorogenic acid at a dosage of 3mg per kilogram of body weight via intramuscular injection. The regimen of chlorogenic acid was once daily for 28 consecutive days, followed by a 7-day drug holiday. From June 2021 to March 2022, patients tolerated chlorogenic acid well and no hepatic or renal impairment or other serious adverse reactions were observed. Karnofsky Performance Status (KPS) score remained ≥ 70 . The patient exhibited some concomitant symptoms, including dysarthria, memory and calculation decline, indistinct speech, and muscle strength of grade III in the right limbs, all of which were considered related to postoperative cerebral edema and not related to drug treatment. Long-term follow-up of the patient was conducted, and Magnetic Resonance Imaging (MRI) were assessed according to the Response Assessment in Neuro-Oncology (RANO) criteria (**Error! Reference source not found.**). Prior to treatment, the patient's MRI showed a large area of signal intensity in the left frontal lobe and splenium of the corpus callosum on Fluid-Attenuated Inversion Recovery (FLAIR), with unclear boundaries, and multiple irregular ring enhancements on T1 Post-Gadolinium (T1WI+C). During mid-treatment (September 2021; March 2022), the FLAIR sequences revealed signal intensity areas around the postoperative cavity, which had significantly reduced compared to pre-treatment, and the irregular enhancement range on T1WI+C had also decreased markedly, with the treatment effect assessed as partial response (PR). Follow-up MRI in 2023 showed further reduction of the abnormal area, with the disappearance of irregular enhancement areas on T1WI+C. The patient continued the chlorogenic acid treatment until January 2024, with monthly follow-ups indicating good patient condition and no new symptoms during the treatment period, after which the patient discontinued the medication voluntarily. In summary, our clinical data demonstrate that chlorogenic acid has a good therapeutic effect against glioma, providing support for the further development of drugs for the treatment of glioma.

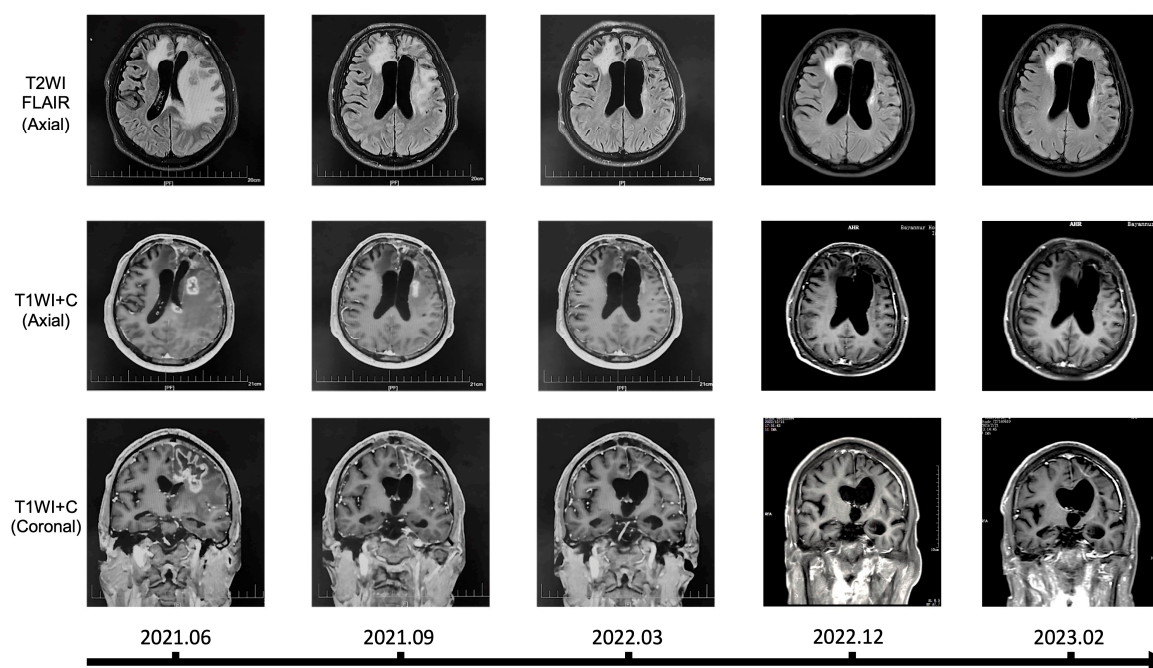


Figure 8. Magnetic resonance imaging (MRI) findings over time in a patient treated with chlorogenic acid.

4. Discussion

TAMs, encompassing myeloid cells and microglia, are extensively enriched in gliomas. Myeloid cells exhibit potent suppressive properties, while microglia tend to have pro-inflammatory inclinations [38]. Utilizing pseudotime analysis, we dissected the transition from bone marrow-derived monocytes to macrophages, a process accompanied by a decrease in the expression of IFN pathway genes and a rapid increase in the expression of the pro-angiogenic factor Vegfa. This culminates in the formation of a suppressive population characterized by high expression of Gpnmb and Apoe genes, marking the completion of the tumor's "hijacking" of monocytes. Traditional views suggest that macrophages can polarize into M1 and M2 types, but newer perspectives widely regard macrophage polarization as a continuous process [8]. As anticipated, the TAM3 subset (Gpnmb+, Apoe+) is more similar to the previously recognized M2 macrophages, while the TAM1 subset resembles M1 type but still expresses a subset of tumor-suppressive genes, reflecting the broad heterogeneity of this population. Microglia surrounding the tumor exhibit activation of the IFN pathway, enhanced expression of MHC-II, and display active transcription factors and cytokines during their activation process, findings consistent with Ochoa's conclusions [38,39]. Therefore, microglia are likely an effective force against tumors in the early stages but may gradually "decline" as the number of blood-derived NK cells, T cells, BMDMs, and other cells increases, thereby losing their ability to resist the tumor. However, further experimental evidence is needed to elucidate how tumors "hijacking" the immune microenvironment.

The biological activities of chlorogenic acid are extensive, including antimicrobial activity, anti-autoimmune disease, and metabolic regulation [41–43]. Early studies have largely focused on the direct cytotoxicity of chlorogenic acid. Gupta et al. systematically reviewed the mechanisms of chlorogenic acid's antitumor effects, which include inducing apoptosis, oxidative stress, affecting tumor's proliferation and migration, and anti-angiogenesis, while more recent studies have begun to focus on the immunomodulatory functions and anticancer mechanisms of chlorogenic acid [44]. Our research, through a series of animal model experiments, has revealed the key role of chlorogenic acid in regulating the function of macrophages and microglia. Our early findings indicated that chlorogenic acid could promote the repolarization of M2-type macrophages to the M1 phenotype, with chlorogenic acid modulating macrophage polarization by promoting and inhibiting the

activation of STAT1 and STAT6 pathways, respectively [16]. We observed that chlorogenic acid could significantly extend the survival of model mice and exert its antitumor effects by regulating the state of tumor-associated macrophages and microglia. GSEA showed that chlorogenic acid activated a series of gene pathways closely related to adaptive immune responses. Notably, chlorogenic acid significantly enhanced the antigen-presenting function of macrophages and the expression of genes related to T-cell immune activation, demonstrating a high degree of congruence with adaptive immunity. Our previous target predictions suggested that the targets of chlorogenic acid on glioma cells might be related to the JAK-STAT and NF- κ B pathways [45]. Li et al. found that in melanoma model mice treated with chlorogenic acid, the proportion of M2-TAMs and CD4-Foxp3+ T cells significantly decreased, while the proportion and activity of CD8+ T cells and M1-TAMs markedly increased [46], a mechanism closely related to the JAK-pSTAT1-IRF1 pathway [18]. Additionally, chlorogenic acid can reduce STAT3 phosphorylation, the protein levels of STAT3 and Snail, block the STAT3/Snail pathway, inhibit the progression of osteosarcoma cells, and induce apoptosis [47]. These conclusions all imply that the JNK-STAT pathway is a key target of chlorogenic acid in the treatment of tumors. With the aid of single-cell sequencing, PPI network analysis, and molecular docking, we propose for the first time that chlorogenic acid activates microglia through STAT1. STAT1 is a key transcription factor widely involved in interferon signaling pathways and JAK-STAT signaling pathways, which play a crucial role in regulating the activation, proliferation, and differentiation of immune cells. Therefore, we believe that improving the function of microglia could potentially benefit patients.

Chlorogenic acid now possesses the potential for clinical application. Our patient data demonstrate the good safety profile of chlorogenic acid, while also showing remarkable therapeutic efficacy. There are currently multiple ongoing clinical trials investigating the use of chlorogenic acid for cancer treatment (NCT03751592, NCT02245204, NCT02136342). Our center has initiated a Phase I clinical trial (CTR20160113) on the treatment of advanced glioma with chlorogenic acid, which has proven its reliable safety and certain therapeutic effects. Chlorogenic acid is currently the subject of a "Phase II/III study evaluating the safety and efficacy of injectable chlorogenic acid in the treatment of recurrent grade IV glioblastoma" (CTR20181644), which will provide more reliable evidence for the clinical efficacy of chlorogenic acid.

5. Conclusions

In summary, we can conclude that the JAK-STAT pathway is the core molecular link between myeloid cells, microglia in the glioma microenvironment, and the mechanism of action of chlorogenic acid. Our findings refine the details of how chlorogenic acid modulates immunity to treat glioma at the RNA and single-cell levels, and demonstrate promising antitumor efficacy in animal models. Our case data also highlight the immense potential of chlorogenic acid for clinical application. This research outcome provides robust support and new insights for drug development, and further establishes a theoretical foundation for the clinical development of chlorogenic acid for the treatment of glioma patients.

6. Patents

Not applicable.

Supplementary Materials: The following supporting information can be downloaded at the website of this paper posted on Preprints.org, Figure S1; Table S1; Table S2; Table S3; Table S4.

Author Contributions: Conceptualization: Jiachen Wang, Shenglan Li, Yuxiao Chen, Wenbin Li. Methodology: Jiachen Wang, Yuxiao Chen, Jinyi Chen, Can Wang, Shenglan Li, Mengqian Huang. Formal analysis: Jiachen Wang, Yuxiao Chen. Visualization: Jiachen Wang, Yuxiao Chen. Writing (original draft): Jiachen Wang, Yuxiao Chen. Writing (Review and editing): Jiachen Wang, Yuxiao Chen, Shenglan Li, Jinyi Chen, Mengqian Huang, Can Wang, Zehao Cai, Yuxiang Fan, Yanjie Lan, Ruining Bai, Yumeng Yu, Feng Chen, Wenbin Li. The work reported in the paper has been performed by the authors, unless clearly specified in the text.

Funding: This research was funded by Talent Introduction Fund of Beijing Tiantan Hospital (RCYJ-2020-2025-LWB), the Beijing Clinical Key Specialty Project (2-1-2-038).

Institutional Review Board Statement: The research involving human participants was conducted in accordance with the approval of the Ethics Committee of Beijing Tiantan Hospital, affiliated with Capital Medical University. We obtained written informed consent from all participants in accordance with the principles outlined in the Declaration of Helsinki. All animal experiments were conducted following the "Guide for the Care and Use of Laboratory Animals" and were approved by the Animal Care and Use Committee.

Informed Consent Statement: This study has obtained written informed consent from the patient for the use of their disease information and imaging results for research and educational purposes. The patient has fully understood and consented to the inclusion of their non-identifiable disease data in the study and its potential publication in academic literature. The research adheres to all relevant privacy protection and ethical standards.

Data Availability Statement: The data that support the findings of this study are available in the supplementary material of this article. Raw 10X single-cell sequencing data are available on request to the authors.

Acknowledgments: Not applicable.

Conflicts of Interest: The authors declare no conflicts of interest.

References

- Weller, M.; Wen, P.Y.; Chang, S.M.; Dirven, L.; Lim, M.; Monje, M.; Reifenberger, G. Glioma. *Nat Rev Dis Primers* **2024**, *10*, 33. <https://doi.org/10.1038/s41572-024-00516-y>.
- Ostrom, Q.T.; Price, M.; Neff, C.; Cioffi, G.; Waite, K.A.; Kruchko, C.; Barnholtz-Sloan, J.S. CBTRUS Statistical Report: Primary Brain and Other Central Nervous System Tumors Diagnosed in the United States in 2016-2020. *Neuro Oncol* **2023**, *25*, iv1-iv99. <https://doi.org/10.1093/neuonc/noad149>.
- Yasinjan, F.; Xing, Y.; Geng, H.; Guo, R.; Yang, L.; Liu, Z.; Wang, H. Immunotherapy: a promising approach for glioma treatment. *Front Immunol* **2023**, *14*, 1255611. <https://doi.org/10.3389/fimmu.2023.1255611>.
- Xing, Y.; Yasinjan, F.; Geng, H.; He, M.; Yang, M.; Gao, Y.; Zhang, J.; Zhang, L.; Guo, B. A scientometric analysis of immunotherapies for gliomas: Focus on GBM. *Asian J Surg* **2024**. <https://doi.org/10.1016/j.asjsur.2024.02.138>.
- Yin, J.; Valin, K.L.; Dixon, M.L.; Leavenworth, J.W. The Role of Microglia and Macrophages in CNS Homeostasis, Autoimmunity, and Cancer. *J Immunol Res* **2017**, *2017*, 5150678. <https://doi.org/10.1155/2017/5150678>.
- Hambardzumyan, D.; Gutmann, D.H.; Kettenmann, H. The role of microglia and macrophages in glioma maintenance and progression. *Nature Neuroscience* **2015**, *19*, 20-27.
- Musca, B.; Russo, M.G.; Tushe, A.; Magri, S.; Battaggia, G.; Pinton, L.; Bonaudo, C.; Della Puppa, A.; Mandruzzato, S. The immune cell landscape of glioblastoma patients highlights a myeloid-enriched and immune suppressed microenvironment compared to metastatic brain tumors. *Front Immunol* **2023**, *14*, 1236824. <https://doi.org/10.3389/fimmu.2023.1236824>.
- Wang, J.; Li, S.; Lan, Y.; Liu, X.; Li, W. Glioma-associated macrophages: unraveling their dual role in the microenvironment and therapeutic implications. *Current Medicine* **2024**.
- Huang, J.; Xie, M.; He, L.; Song, X.; Cao, T. Chlorogenic acid: a review on its mechanisms of anti-inflammation, disease treatment, and related delivery systems. *Front Pharmacol* **2023**, *14*, 1218015. <https://doi.org/10.3389/fphar.2023.1218015>.
- Huang, S.; Wang, L.L.; Xue, N.N.; Li, C.; Guo, H.H.; Ren, T.K.; Zhan, Y.; Li, W.B.; Zhang, J.; Chen, X.G.; et al. Chlorogenic acid effectively treats cancers through induction of cancer cell differentiation. *Theranostics* **2019**, *9*, 6745-6763. <https://doi.org/10.7150/thno.34674>.
- Gupta, A.; Atanasov, A.G.; Li, Y.; Kumar, N.; Bishayee, A. Chlorogenic acid for cancer prevention and therapy: Current status on efficacy and mechanisms of action. *Pharmacol Res* **2022**, *186*, 106505. <https://doi.org/10.1016/j.phrs.2022.106505>.
- Nwafor, E.-O.; Lu, P.; Zhang, Y.; Liu, R.; Peng, H.; Xing, B.; Liu, Y.; Li, Z.; Zhang, K.; Zhang, Y.; et al. Chlorogenic acid: Potential source of natural drugs for the therapeutics of fibrosis and cancer. *Transl Oncol* **2022**, *15*, 101294. <https://doi.org/10.1016/j.tranon.2021.101294>.
- Skąła, E.; Kowalczyk, T.; Toma, M.; Szemraj, J.; Radek, M.; Pytel, D.; Wiczfinska, J.; Wysokińska, H.; Śliwiński, T.; Sitarek, P. Induction of apoptosis in human glioma cell lines of various grades through the ROS-mediated mitochondrial pathway and caspase activation by Rhaponticum carthamoides transformed root extract. *Mol Cell Biochem* **2018**, *445*, 89-97. <https://doi.org/10.1007/s11010-017-3254-z>.
- Skąła, E.; Sitarek, P.; Toma, M.; Szemraj, J.; Radek, M.; Nieborowska-Skorska, M.; Skorski, T.; Wysokińska, H.; Śliwiński, T. Inhibition of human glioma cell proliferation by altered Bax/Bcl-2-p53 expression and apoptosis induction by Rhaponticum carthamoides extracts from transformed and normal roots. *J Pharm Pharmacol* **2016**, *68*, 1454-1464. <https://doi.org/10.1111/jphp.12619>.

15. Sitarek, P.; Skala, E.; Toma, M.; Wielanek, M.; Szemraj, J.; Skorski, T.; Bialas, A.J.; Sakowicz, T.; Kowalczyk, T.; Radek, M.; et al. Transformed Root Extract of *Leonurus sibiricus* Induces Apoptosis through Intrinsic and Extrinsic Pathways in Various Grades of Human Glioma Cells. *Pathol Oncol Res* **2017**, *23*, 679-687. <https://doi.org/10.1007/s12253-016-0170-6>.
16. Xue, N.; Zhou, Q.; Ji, M.; Jin, J.; Lai, F.; Chen, J.; Zhang, M.; Jia, J.; Yang, H.; Zhang, J.; et al. Chlorogenic acid inhibits glioblastoma growth through repolarizing macrophage from M2 to M1 phenotype. *Sci Rep* **2017**, *7*, 39011. <https://doi.org/10.1038/srep39011>.
17. Ye, J.; Yang, Y.; Jin, J.; Ji, M.; Gao, Y.; Feng, Y.; Wang, H.; Chen, X.; Liu, Y. Targeted delivery of chlorogenic acid by mannosylated liposomes to effectively promote the polarization of TAMs for the treatment of glioblastoma. *Bioact Mater* **2020**, *5*, 694-708. <https://doi.org/10.1016/j.bioactmat.2020.05.001>.
18. Li, R.; Zhan, Y.; Ding, X.; Cui, J.; Han, Y.; Zhang, J.; Zhang, J.; Li, W.; Wang, L.; Jiang, J. Cancer Differentiation Inducer Chlorogenic Acid Suppresses PD-L1 Expression and Boosts Antitumor Immunity of PD-1 Antibody. *Int J Biol Sci* **2024**, *20*, 61-77. <https://doi.org/10.7150/ijbs.83599>.
19. Zhang, Y.; Yang, Y.; Ye, J.; Gao, Y.; Liao, H.; Zhou, J.; Feng, Y.; Liu, D.; Meng, Y.; Chen, X.; et al. Construction of chlorogenic acid-containing liposomes with prolonged antitumor immunity based on T cell regulation. *Sci China Life Sci* **2021**, *64*, 1097-1115. <https://doi.org/10.1007/s11427-020-1739-6>.
20. Kang, Z.; Li, S.; Kang, X.; Deng, J.; Yang, H.; Chen, F.; Jiang, J.; Zhang, J.; Li, W. Phase I study of chlorogenic acid injection for recurrent high-grade glioma with long-term follow-up. *Cancer Biol Med* **2023**, *20*, 465-476. <https://doi.org/10.20892/j.issn.2095-3941.2022.0762>.
21. Zheng, G.X.; Terry, J.M.; Belgrader, P.; Ryvkin, P.; Bent, Z.W.; Wilson, R.; Ziraldo, S.B.; Wheeler, T.D.; McDermott, G.P.; Zhu, J.; et al. Massively parallel digital transcriptional profiling of single cells. *Nat Commun* **2017**, *8*, 14049. <https://doi.org/10.1038/ncomms14049>.
22. Stuart, T.; Butler, A.; Hoffman, P.; Hafemeister, C.; Papalexi, E.; Mauck, W.M., 3rd; Hao, Y.; Stoeckius, M.; Smibert, P.; Satija, R. Comprehensive Integration of Single-Cell Data. *Cell* **2019**, *177*, 1888-1902.e1821. <https://doi.org/10.1016/j.cell.2019.05.031>.
23. Hao, Y.; Hao, S.; Andersen-Nissen, E.; Mauck, W.M., 3rd; Zheng, S.; Butler, A.; Lee, M.J.; Wilk, A.J.; Darby, C.; Zager, M.; et al. Integrated analysis of multimodal single-cell data. *Cell* **2021**, *184*, 3573-3587.e3529. <https://doi.org/10.1016/j.cell.2021.04.048>.
24. Korsunsky, I.; Millard, N.; Fan, J.; Slowikowski, K.; Zhang, F.; Wei, K.; Baglaenko, Y.; Brenner, M.; Loh, P.R.; Raychaudhuri, S. Fast, sensitive and accurate integration of single-cell data with Harmony. *Nat Methods* **2019**, *16*, 1289-1296. <https://doi.org/10.1038/s41592-019-0619-0>.
25. Wu, T.; Hu, E.; Xu, S.; Chen, M.; Guo, P.; Dai, Z.; Feng, T.; Zhou, L.; Tang, W.; Zhan, L.; et al. clusterProfiler 4.0: A universal enrichment tool for interpreting omics data. *Innovation (Camb)* **2021**, *2*, 100141. <https://doi.org/10.1016/j.xinn.2021.100141>.
26. The Gene Ontology Resource: 20 years and still GOing strong. *Nucleic Acids Res* **2019**, *47*, D330-d338. <https://doi.org/10.1093/nar/gky1055>.
27. M, C. org.Mm.eg.db: Genome wide annotation for Mouse. R package version 3.8.2. **2019**.
28. Trapnell, C.; Cacchiarelli, D.; Grimsby, J.; Pokharel, P.; Li, S.; Morse, M.; Lennon, N.J.; Livak, K.J.; Mikkelsen, T.S.; Rinn, J.L. The dynamics and regulators of cell fate decisions are revealed by pseudotemporal ordering of single cells. *Nat Biotechnol* **2014**, *32*, 381-386. <https://doi.org/10.1038/nbt.2859>.
29. Hänzelmann, S.; Castelo, R.; Guinney, J. GSVA: gene set variation analysis for microarray and RNA-seq data. *BMC Bioinformatics* **2013**, *14*, 7. <https://doi.org/10.1186/1471-2105-14-7>.
30. Kim, S.; Chen, J.; Cheng, T.; Gindulyte, A.; He, J.; He, S.; Li, Q.; Shoemaker, B.A.; Thiessen, P.A.; Yu, B.; et al. PubChem in 2021: new data content and improved web interfaces. *Nucleic Acids Res* **2021**, *49*, D1388-d1395. <https://doi.org/10.1093/nar/gkaa971>.
31. Daina, A.; Michielin, O.; Zoete, V. SwissTargetPrediction: updated data and new features for efficient prediction of protein targets of small molecules. *Nucleic Acids Research* **2019**, *47*, W357-W364. <https://doi.org/10.1093/nar/gkz382>.
32. Gallo, K.; Goede, A.; Preissner, R.; Gohlke, B.O. SuperPred 3.0: drug classification and target prediction-a machine learning approach. *Nucleic Acids Res* **2022**, *50*, W726-w731. <https://doi.org/10.1093/nar/gkac297>.
33. Amberger, J.S.; Hamosh, A. Searching Online Mendelian Inheritance in Man (OMIM): A Knowledgebase of Human Genes and Genetic Phenotypes. *Curr Protoc Bioinformatics* **2017**, *58*, 1.2.1-1.2.12. <https://doi.org/10.1002/cpbi.27>.
34. Stelzer, G.; Rosen, N.; Plaschkes, I.; Zimmerman, S.; Twik, M.; Fishilevich, S.; Stein, T.I.; Nudel, R.; Lieder, I.; Mazor, Y.; et al. The GeneCards Suite: From Gene Data Mining to Disease Genome Sequence Analyses. *Curr Protoc Bioinformatics* **2016**, *54*, 1.30.31-31.30.33. <https://doi.org/10.1002/cpbi.5>.
35. Chin, C.H.; Chen, S.H.; Wu, H.H.; Ho, C.W.; Ko, M.T.; Lin, C.Y. cytoHubba: identifying hub objects and sub-networks from complex interactome. *BMC Syst Biol* **2014**, *8 Suppl 4*, S11. <https://doi.org/10.1186/1752-0509-8-s4-s11>.

36. Ru, J.; Li, P.; Wang, J.; Zhou, W.; Li, B.; Huang, C.; Li, P.; Guo, Z.; Tao, W.; Yang, Y.; et al. TCMSP: a database of systems pharmacology for drug discovery from herbal medicines. *J Cheminform* **2014**, *6*, 13. <https://doi.org/10.1186/1758-2946-6-13>.
37. Berman, H.M.; Westbrook, J.; Feng, Z.; Gilliland, G.; Bhat, T.N.; Weissig, H.; Shindyalov, I.N.; Bourne, P.E. The Protein Data Bank. *Nucleic Acids Res* **2000**, *28*, 235-242. <https://doi.org/10.1093/nar/28.1.235>.
38. Ochocka, N.; Segit, P.; Wojnicki, K.; Cyranowski, S.; Swatler, J.; Jacek, K.; Grajkowska, W.; Kaminska, B. Specialized functions and sexual dimorphism explain the functional diversity of the myeloid populations during glioma progression. *Cell Rep* **2023**, *42*, 111971. <https://doi.org/10.1016/j.celrep.2022.111971>.
39. Ochocka, N.; Segit, P.; Walentynowicz, K.A.; Wojnicki, K.; Cyranowski, S.; Swatler, J.; Mieczkowski, J.; Kaminska, B. Single-cell RNA sequencing reveals functional heterogeneity of glioma-associated brain macrophages. *Nat Commun* **2021**, *12*, 1151. <https://doi.org/10.1038/s41467-021-21407-w>.
40. Kirschenbaum, D.; Xie, K.; Ingelfinger, F.; Katzenelenbogen, Y.; Abadie, K.; Look, T.; Sheban, F.; Phan, T.S.; Li, B.; Zwicky, P.; et al. Time-resolved single-cell transcriptomics defines immune trajectories in glioblastoma. *Cell* **2024**, *187*, 149-165.e123. <https://doi.org/10.1016/j.cell.2023.11.032>.
41. Santana-Gálvez, J.; Cisneros-Zevallos, L.; Jacobo-Velázquez, D.A. Chlorogenic Acid: Recent Advances on Its Dual Role as a Food Additive and a Nutraceutical against Metabolic Syndrome. *Molecules* **2017**, *22*. <https://doi.org/10.3390/molecules22030358>.
42. Zheng, C.; Zhong, Y.; Zhang, W.; Wang, Z.; Xiao, H.; Zhang, W.; Xie, J.; Peng, X.; Luo, J.; Xu, W. Chlorogenic Acid Ameliorates Post-Infectious Irritable Bowel Syndrome by Regulating Extracellular Vesicles of Gut Microbes. *Adv Sci (Weinh)* **2023**, *10*, e2302798. <https://doi.org/10.1002/advs.202302798>.
43. Pimpley, V.; Patil, S.; Srinivasan, K.; Desai, N.; Murthy, P.S. The chemistry of chlorogenic acid from green coffee and its role in attenuation of obesity and diabetes. *Prep Biochem Biotechnol* **2020**, *50*, 969-978. <https://doi.org/10.1080/10826068.2020.1786699>.
44. Gupta, A.; Atanasov, A.G.; Li, Y.; Kumar, N.; Bishayee, A. Chlorogenic acid for cancer prevention and therapy: Current status on efficacy and mechanisms of action. *Pharmacol Res* **2022**, *186*, 106505. <https://doi.org/10.1016/j.phrs.2022.106505>.
45. Ren, T.; Wang, Y.; Wang, C.; Zhang, M.; Huang, W.; Jiang, J.; Li, W.; Zhang, J. Isolation and identification of human metabolites from a novel anti-tumor candidate drug 5-chlorogenic acid injection by HPLC-HRMS/MS(n) and HPLC-SPE-NMR. *Anal Bioanal Chem* **2017**, *409*, 7035-7048. <https://doi.org/10.1007/s00216-017-0657-3>.
46. Li, X.; Zhu, S.; Yin, P.; Zhang, S.; Xu, J.; Zhang, Q.; Shi, S.; Zhang, T. Combination immunotherapy of chlorogenic acid liposomes modified with sialic acid and PD-1 blockers effectively enhances the anti-tumor immune response and therapeutic effects. *Drug Deliv* **2021**, *28*, 1849-1860. <https://doi.org/10.1080/10717544.2021.1971797>.
47. Zhang, F.; Yin, G.; Han, X.; Jiang, X.; Bao, Z. Chlorogenic acid inhibits osteosarcoma carcinogenesis via suppressing the STAT3/Snail pathway. *J Cell Biochem* **2019**, *120*, 10342-10350. <https://doi.org/10.1002/jcb.28318>.

Disclaimer/Publisher's Note: The statements, opinions and data contained in all publications are solely those of the individual author(s) and contributor(s) and not of MDPI and/or the editor(s). MDPI and/or the editor(s) disclaim responsibility for any injury to people or property resulting from any ideas, methods, instructions or products referred to in the content.